Nanoscale

# Silver Nanoparticle Film Induced Photoluminescence Enhancement of Near-infrared Emitting PbS and PbS/CdS Core/shell Quantum Dots: Observation of Different Enhancement Mechanisms



| | |
|---|---|
| Journal: | *Nanoscale* |
| Manuscript ID | NR-COM-08-2015-005906.R1 |
| Article Type: | Communication |
| Date Submitted by the Author: | 24-Dec-2015 |
| Complete List of Authors: | Liang, Hongyan; INRS, EMT<br>Zhao, Haiguang; INRS,<br>Li, Zhipeng; Capital Normal University, Department of Physics<br>Harnagea, Catalin; INRS, Univ. of Quebec, Energy, Materials and Telecommunications<br>Ma, Dongling; INRS, EMT |
| | |

Nanoscale

COMMUNICATION

# Silver Nanoparticle Film Induced Photoluminescence Enhancement of Near-infrared Emitting PbS and PbS/CdS Core/shell Quantum Dots: Observation of Different Enhancement Mechanisms

Received 00th January 20xx,
Accepted 00th January 20xx

DOI: 10.1039/x0xx00000x

www.rsc.org/

H.Y. Liang,[a] H.G. Zhao,*[a] Z.P. Li,[b] C. Harnagea,[a] and D.L. Ma *[a]

**Ag nanoparticles and near-infrared quantum dots (QDs) plasmon/fluorophore system is investigated for photoluminescence (PL) enhancement. By tuning surface plasmon resonance of the Ag film and PL bands of the QDs, enhancement mechanisms and enhancement factors (EF) were varied. Optimization of experimental parameters led to a maximum EF of 2.8.**

Colloidal quantum dots (QDs) have drawn increasing attention due to their unique size-dependent optical properties, which are attractive in a variety of potential applications.[1, 2] Among all kinds of QDs, lead chalcogenide QDs have both large excitation Bohr radii and small bulk band gaps, thus allowing quantum confinement in relatively large sized QDs simultaneously with a tunable near-infrared (NIR) emission.[1, 2] Potential applications of these QDs include NIR photodetectors, light-emitting diodes, biosensors and solar cells.[1, 2] For most of these applications, it is desired yet challenging to obtain lead calcogenide QD film with excellent and stable optical and optoelectronic properties even under ambient atmosphere. One of the major problems that has hampered some of their practical implementation is that the quantum yield (QY) of lead chalcogenide QDs decreases significantly during film deposition and/or device fabrication, due to their surface oxidation, introduction of new surface defects/trap states, quenching by species in their environments or energy transfer among themselves.[3] Aiming to address this issue, recently, researchers have widely studied the fluorescence behaviour of visible (Vis)-emitting QDs interacting with surface plasmon resonance (SPR) of metallic nanostructures, which hold great promise to enhance the photoluminescence (PL) of QDs.[4-7] Plasmonic metallic nanostructures can act as nanoscopic antennas to induce the redistribution of local photonic mode density, and concentrate and confine electromagnetic energy into small volumes below the optical diffraction limitation.[8] Fluorophores located in the vicinity of metallic nanostructures interact with them, resulting in modifications of the excitation/emission behaviour of the fluorophores.[9-11] The strength of the interactions depends on the degree of overlap of the SPR band with the absorption and/or emission band of fluorophores, as well as the distance between plasmonic structures and fluorophores.[12] The plasmon/fluorophore interactions can mainly lead to three effects: excitation enhancement (increase of excitation rate and thus enhanced absorption), emission enhancement (increase of radiative decay rate and thus emission amplification) and quenching (increase of nonradiative decay rate and thus reduced emission).[7,13-16] Overall, the final PL performance of fluorophores is determined by the competition between enhancement and quenching effects, which further depends on the particular plasmon/fluorophore system. Understanding the behaviour of plasmon/fluorophore interactions requires extensive investigations through varying multiple experimental parameters, such as plasmonic resonance features and emission wavelengths, crucial for the advancement of theoretical investigations and for practical applications.

The PL enhancement of Vis-emitting QDs using plasmonic structures has been investigated extensively.[6,12-13] In these cases, usually the excitation wavelength is close to the emission peak wavelength and thus both excitation and emission enhancement mechanisms are induced simultaneously since the SPR band of plasmonic nanostructures can be readily designed to cover both the excitation and emission wavelengths.[15, 16] In comparison, NIR-emitting lead calcogenide QDs can be excited with Vis lights and the wavelength difference between the excitation and emission can be adjusted in a quite large wavelength range that makes it interesting to separate and study different enhancement mechanisms. Up to now, the reports related to

[a] *Institut National de la Recherche Scientifique, University of Québec, 1650 Boulevard Lionel-Boulet, Varennes, Québec, J3X 1S2 Canada.*
[b] *Beijing Key Laboratory of Nano-Photonics and Nano-Structure (NPNS), Department of Physics, Capital Normal University, Beijing, 100048 China*
* Corresponding authors: zhaoh@emt.inrs.ca and ma@emt.inrs.ca
Electronic Supplementary Information (ESI) available: [Experiments, SEM images, calculation results, typical PL spectra under different exication and PL decay curves for PbS/CdS QDs with and without Ag#2 at different conditions]. See DOI: 10.1039/x0xx00000x

the PL enhancement of lead calcogenide QDs through plasmonic nanostructures remain very limited. In one case, Tanaka et al, have studied the PL enhancement of PbS QDs via coupling them with metallic materials.[17] In their investigation, a plasmonic antenna was produced by focused ion beam, a time-consuming and costly technique. In addition, the SPR peak only matches the emission peak of PbS QDs. It is still challenging to achieve the PL enhancement of PbS-based QDs through both the excitation and emission enhancement.

In this work, we not only present a facile and inexpensive approach (that does not involve expansive lithography processes for fabricating plasmonic structures) for further enhancing the PL of high-quality PbS-based QDs, but also investigate the PL enhancement mechanisms by tuning the excitation wavelength and the overlap between SPR and QDs' emission bands. Beside PbS QDs, core/shell PbS/CdS QDs that showed high QY and good thermal- and photo-stability were also used as fluorophores.[18] Ag nanoparticle (NP) films with single or double SPR bands were used to enhance the PL under different excitation wavelengths. At the same time, fluorescence lifetime was measured to understand the enhancement mechanism. The optimal QDs/Ag film showed a remarkable ~2.8-fold PL enhancement over the Ag-absent QD film. It was found that when the Ag film with a single SPR peak in the Vis range was used, the PL enhancement was dominated by the excitation enhancement in the investigated wavelength range of excitation. Interestingly, for the Ag film with two SPR bands, the PL enhancement mechanisms varied with excitation wavelength. When excitation wavelength was set at 444 nm, only the excitation enhancement was manifest. However, when excitation wavelength was 636 nm, both excitation and emission enhancement contributed to the PL enhancement as evidenced by a larger enhancement factor (EF) as well as by a shorter lifetime. The results are intriguing as the emission enhancement is supposed to be independent of the excitation wavelength, and to depend solely on the overlap of the PL band with the SPR band, where resonances can be excited by the PL of QDs.[14] We propose that the excitation wavelength-dependent PL enhancement and mechanisms can arise from different coupling efficiency between the QDs and plasmon modes. These findings could be helpful for the application of luminescent PbS-based QD films and for understanding their PL enhancement in general.

PbS[19,20] and PbS/CdS[18] core/shell QDs and colloidal Ag NPs,[21-24] were synthesized through established protocols. QD/Ag films were prepared via a layer-by-layer assemble approach (Fig. 1a). The Ag NPs were firstly deposited on indium tin oxide (ITO)-coated glass slides by drop casting. Then a PMMA film was spin coated on the formed Ag NP film, in order to form the dielectric layer that prohibits PL quenching.[13, 17] The thickness of the PMMA film was ~44 nm, estimated from atomic force microscopy measurements. Lastly, the QDs dispersed in PMMA solution were deposited on the top via spin coating. In order to adjust the plasmon band, two types of Ag NPs capped with different ligands (PVP and EG, or PVP and PEG) were synthesized for preparing a monolayer Ag NP film (Fig. 1b and 1c). The Ag NPs, denoted as Ag#1, had the average diameter of 51 ± 27 nm (Fig. 1b) and those denoted as Ag#2 showed the average size of 72 ± 19 nm (Fig. 1c). All particles were assumed as spheres during scanning electron microscopy (SEM) size measurements. (Fig. S1) The extinction spectra of both Ag samples in solution showed a typical dipolar SPR band (Fig. 1e and f), with single peaks situated at 420 nm and 450 nm, respectively. The red-shift of

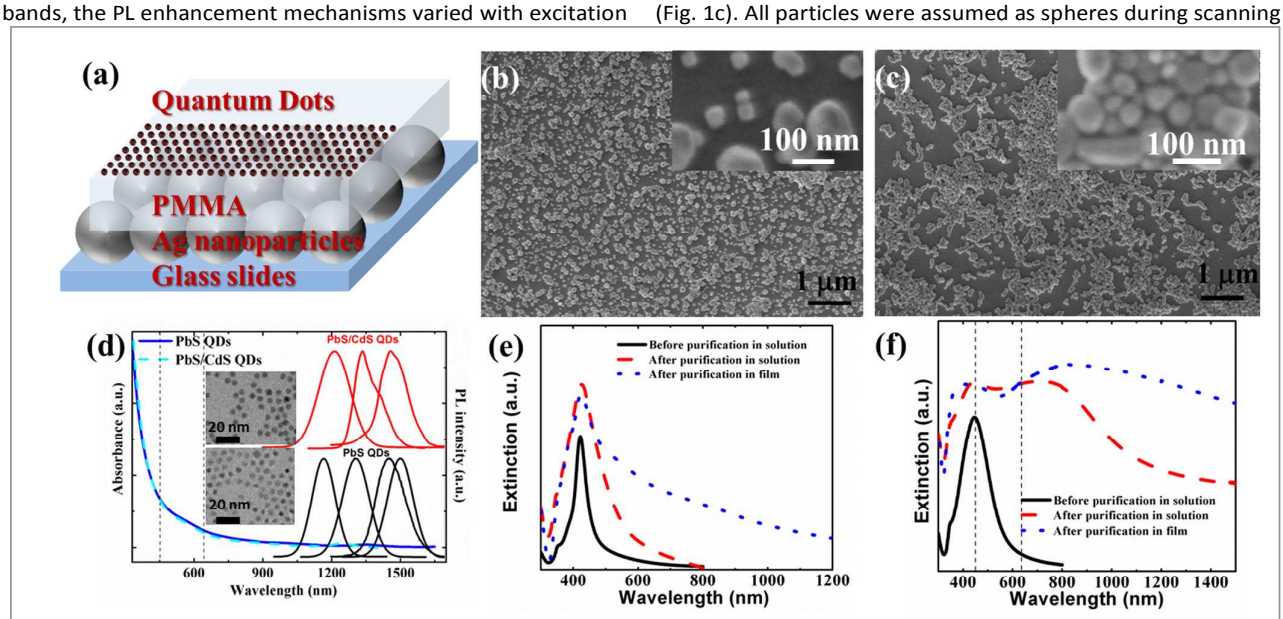


Fig. 1 (a) Schematic illustration of a sample containing QDs on a Ag NP film. SEM images of (b) Ag#1 and (c) Ag#2 films. (d) Absoprtion spectra (left) of PbS and PbS/CdS core/shell QDs with PL peaks at 1500 nm and 1350 nm, respectively, and PL spectra of a series of PbS and PbS/CdS core/shell QDs. Insets: TEM images of PbS/CdS core/shell QDs (top) and PbS QDs (bottom). The extinction spectra of (e) Ag#1 and (f) Ag#2 before and after purification in solution and after film deposition. They are offset for clarity. The dash lines in (d) and (f) denote 450 nm and 636 nm excitation, respectively.

the SPR of Ag#2 with respect to Ag#1 was mainly due to the larger size of Ag#2 NPs. Please note that as different ligands (EG vs PEG) were used and they affected the stability of Ag NPs differently,[25,26] after purification and film deposition, the SPR patterns of Ag#1 and Ag#2 became quite different. The morphology of individual Ag#1 NPs did not change considerably, therefore their SPR peak did not show any significant shift after purification although peak broadening was observed, likely due to slight agglomeration of certain Ag NPs. Film deposition further caused inhomogeneous broadening and the obvious increase of extinction intensity at the longer wavelength side, due to the coupling effect between Ag NPs of different sizes and of different inter-particles distance.[12,27] In particular, the weak SPR edge of Ag#1 (e.g., absorbance at 1200 nm; please note the extinction curves in Fig. 1e and f were offset for clarity) extended into the NIR range was considered to be due to the coupling of a small fraction of Ag NPs with relatively large size, as predicted by theoretical calculations using a simple model based on the coupling of two NPs of the same size (Fig. S2). Basically, the coupling between larger size NPs at shorter inter-particle distance led to more obvious SPR red shift. In a remarkable contrast, purification process of Ag#2 resulted in the appearance of an additional SPR peak at 750 nm (Fig. 1f). This peak was attributed to both the strong plasmon coupling effect of spherical NPs[11,16,28-30] (Fig. S2) and the longitudinal SPR mode in the small fraction of one dimensional (1D) structures (Fig. 1c) formed during the purification process.[23, 24] Once made into the film, the coupling of Ag#2 NPs became even stronger, leading to a strong resonance in the broad NIR range extending up to at least 1500 nm (the maximum wavelength measured herein). This observation was again consistent with theoretical calculation results, although the real case was much more complicated due to the non-uniform size and shape distribution of Ag NPs in Ag#2. Despite this complexity, the SPR spectra of both Ag#1 and Ag#2 films were very reproducible and thus both could serve as suitable substrates for plasmon enhanced PL studies of current interest.

All the NIR emitting QDs used in this investigation showed narrow size distribution (Fig. 1d insets), high QY and good stability in solution. The QY in toluene ranged in between 19~ 85% for PbS QDs and 36~ 52% for PbS/CdS QDs, depending on their emission wavelengths (Table S1).[18,20] When the emission wavelength was similar, the PbS/CdS QDs showed significantly higher QY, indicating their higher optical quality, as expected. After deposition on the substrate, the emission peak wavelength of QDs did not significantly change but the relevant PL intensity dropped. Also, these QDs showed broad absorption and a narrow PL peak. The typical PL spectra of PbS and PbS/CdS QDs with PL peak wavelength ranging from 1100 to 1500 nm are shown in Fig. 1d. By choosing different QDs and Ag NP films, we could alter the overlap of the emission peak of the QDs with the SPR band of Ag NPs.

The as-prepared Ag NPs film was nearly monolayer (Fig. 1b and 1c). With same spin-coating conditions, the concentration and distribution of QDs in the PMMA film should be similar, which made it possible to study their PL intensity variation with the introduction of the Ag NPs layer underneath. PL intensities of PbS QDs with an emission peak at 1500 nm with/without Ag#1 were collected under tunable excitation wavelengths from 300 to 600 nm, to systematically examine the variation in their emission intensity at different excitation wavelengths (Fig. 2a). The typical PL spectra of this PbS QD sample are shown in Fig. S3. The PL EF (defined as the ratio of the PL intensity of QDs/Ag to that of Ag-absent QDs) versus excitation wavelength and the SPR spectrum of the Ag#1 film are shown in Fig. 2b. The maximum EF (2.4) was found at the excitation wavelength of 450 nm and the shape of EF curve nearly followed that of the extinction spectrum. Intriguingly, the excitation wavelength that induced a maximum EF for QDs was 25 nm off the SPR peak, and the reason is still under investigation. It is worthwhile to point out that, when the excitation wavelength was under 350 nm, the EFs were nearly equal to 1, which further confirmed the number of QDs on both films with/without Ag was similar and comparable. We also measured the PL enhancement with Ag#1 for other PbS and PbS/CdS QDs having different emission wavelength and they basically showed the same trend. The PL EFs for different QDs under 450 nm excitation were summarized in Fig. 2c: the average value was nearly constant for all samples and fell into the range of 1.9~2.2. It may be noted that the EF values are not very high. Quite likely the high QY of QDs investigated herein limits the enhancement effect. To better clarify the enhancement mechanism, we investigated the emission

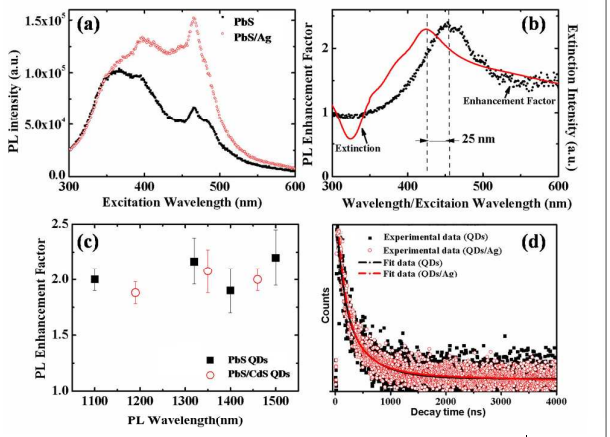


Fig. 2 (a) PL intensity at the emission peak wavelength of 1500 nm of PbS QDs with and without the presence of Ag#1 as a function of excitation wavelength. (b) PL EF of QDs (dots) and the extinction spectrum of Ag#1 (solid line) versus excitation wavelength. (c) PL EF at 450 nm excitation wavelength for different QDs/Ag#1 system. (d) Typical PL decay curves of PbS QDs with and without Ag#1 measured at the emission peak of 1100 nm with a 444 nm laser.

kinetics using time-resolved fluorescence spectroscopy. The representative decay curves of the QDs showing an emission peak at 1100 and 1500 nm are shown in Fig. 2d and Fig. S3b,

respectively. The lifetime did not show any significant change with the presence of the Ag layer for all the investigated QD samples.

The above results demonstrate that the PL enhancement is apparently dependent on the excitation wavelength and insensitive to the emission wavelength. Such an observation is generally explained by the excitation enhancement.[13] It seemed to be a reasonable explanation herein as there was almost no spectral overlap between the SPR of Ag#1 (negligible resonance beyond 1100 nm) and the emission of QDs, which essentially excluded the emission enhancement. The absorption enhancement of PbS QDs due to the presence of a plasmonic scattering layer of Ag NPs has also recently been reported by Arquer et al.[31] The constant lifetimes for QD samples with/without Ag NPs films further confirmed the lacking of the emission enhancement in our system. As a conclusion, the PL enhancement of QDs by combining them with Ag#1 was mainly dominated by the excitation enhancement.

As Ag#2 had two broad SPR bands, one in the Vis range and the other in the NIR range, covering both absorption and emission wavelengths of QDs investigated herein, it was expected to induce both excitation and emission enhancements simultaneously. Since PbS/CdS core/shell QDs showed better stability with respect to PbS QDs,[18] in the following, we concentrate our discussion only on the PbS/CdS core/shell QDs. PL intensities of PbS/CdS QDs with an emission peak at 1190 nm with/without Ag#2 were collected under tunable excitation wavelengths from 300 to 600 nm, to systematically examine the variation in their emission intensity at different excitation wavelenths (Fig. S4). In general, the PL EFs got larger at longer excitation wavelengths. Fig. 3a-c shows the recorded PL spectra of PbS/CdS QDs with/without Ag NPs film under two specific excitation wavelengths of 450 and 636 nm. The PL peak positions of these QDs were located at 1190, 1350 and 1460 nm, respectively. For the purpose of straightforward comparison of the PL enhancement at different excitation, the PL spectra of PbS/CdS QD samples without the presence of Ag#2 were first normalized to their respective peak intensity under each excitation and the spectra of QDs/Ag samples excited at corresponding wavelengths were then modified accordingly. The PL EFs determined from Fig. 3(a) – (c) were 1.8 ± 0.2, 2.1 ± 0.2 and 1.9 ± 0.1 under 450 nm excitation, and 2.8 ± 0.1, 2.5 ± 0.1 and 2.1 ± 0.1 under 636 nm excitation, respectively. Therefore, under 450 nm excitation, there was no significant difference in the EF among three samples, similar to the enhancement behaviour of QDs after their deposition on Ag#1. However, under 636 nm excitation, the case was quite different. The QDs with the emission peak at 1190 nm showed the highest EF while the QDs with 1460 nm emission showed the lowest EF. The emission kinetics of QDs was further investigated using the time-resolved fluorescence decay technique. With the excitation wavelength of 444 nm, the decay curves were indistinguishable for the QDs with and without the presence of

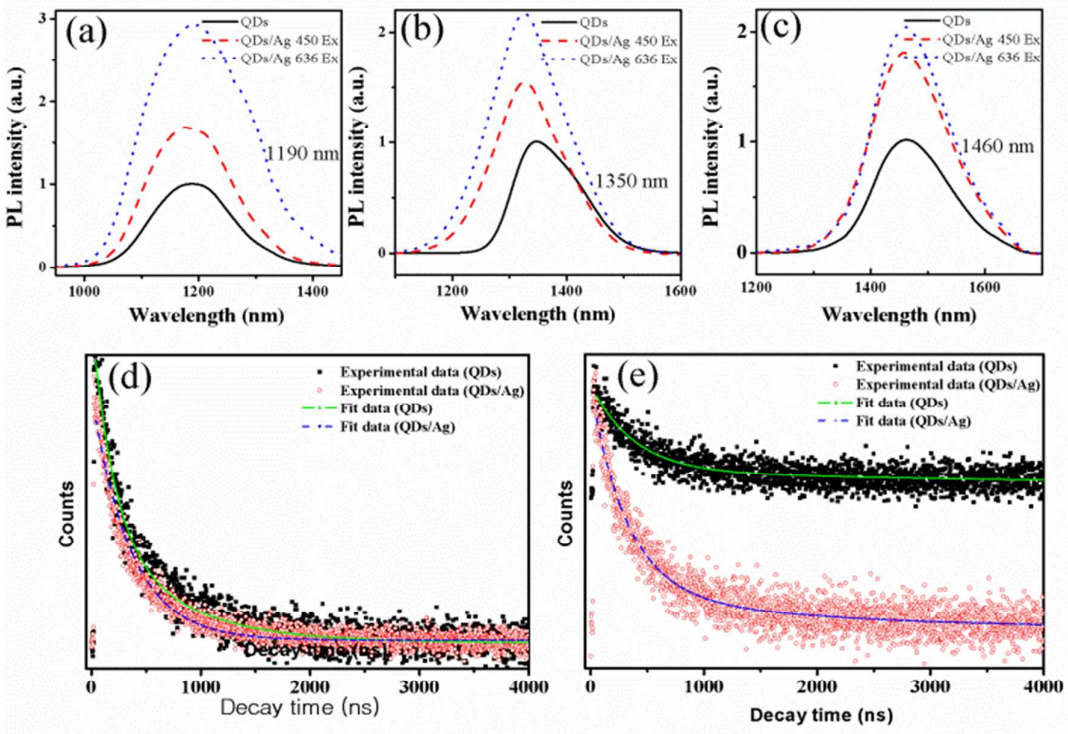


Fig. 3 PL spectra of PbS/CdS QDs alone and those in the presence of Ag#2. The QDs showed emission peaks at (a) 1190 nm, (b) 1350 nm and (c) 1460 nm, respectively. The excitation wavelengths were 450 nm and 636 nm. The PL spectra of Ag-absent QD films under each excitation wavelength were normalized to respective peak intensity. PL decay curves for PbS/CdS QDs with and without Ag#2 measured at the emission peak of 1190 nm with (d) 444 nm and (e) 636 nm lasers.

Ag#2. In contrast, difference was noticed for excitation at 636 nm for all three samples. For QDs/Ag#2 film with an emission peak at 1190 nm, the lifetime was 487 ± 15 ns when they were excited by 444 nm, which represented 98% of that of Ag-absent PbS/CdS QD film. However, it showed 30% reduction compared to that of Ag-absent PbS/CdS QDs (from 497 ± 10 ns to 349 ± 20 ns) under 636 nm excitation (Fig. 3e). Similar phenomena were found for PbS/CdS QD samples with emission peaks at 1350 nm and 1460 nm, although with less variation of the lifetime. As shown in Fig. S5, under the excitation of 636 nm the lifetime of QDs/Ag#2 with an emission peak at 1350 nm changed from 360 ± 10 ns to 300 ± 15 ns (17 % reduction) and with an emission peak at 1460 nm changed from 529 ± 6 ns to 462 ± 25 ns (13 % reduction). It should be emphasized here that the lifetime of Ag-absent PbS/CdS QDs was identical under these two excitation wavelengths. For the QD sample showing the emission peak at 1190 nm, the PL EF under 636 nm excitation increased by a factor of 1.56 when compared to that under 450 nm excitation, which was higher than that of the QD samples with emission peaks at 1350 nm (1.19) and 1460 nm (1.10). These observations indicate that the emission enhancement also contributes to the PL enhancement when the samples are excited at 636 nm, although it does not play an obvious role under 450 nm excitation.

The PL enhancement mechanism under these two excitations was indeed expected to be similar, because both excitations overlap with the absorption of QDs and overlap with the SPR of Ag#2 in the Vis range, but were far away from the emission of QDs and the SPR of Ag#2 in the NIR range. In addition, the PL EFs were also expected to be similar as SPR intensities were almost the same at both excitation wavelengths as shown in Fig. 1. The unexpected variation of PL EFs and lifetime with excitation wavelength can reasonably be explained by the emission enhancement under 636 nm excitation, which results from the interaction between QDs and SPR in the emission range.[14,17] In general, when the excitation wavelength is far away from the SPR in the emission range, the SPR could only be excited by the PL of QDs, and the interaction between the SPR and QDs could modify the radiative decay rate.[14] In our case, because the coupled SPR mode at 636 nm is expected to generate a stronger and larger area local EM field, it highly likely leads to more efficient coupling between the plasmon mode and the QDs and thereby, stronger PL,[17] which further efficiently initiates plasmonic resonances in the PL wavelength range and therefore more efficient interactions between the QDs and related plasmon modes. A similar excitation wavelength-dependent emission enhancement has been found in the system of CdSe/CdS/ZnS core/shell/shell QD/Ag nanoprism. In that case, the presence of higher-order plasmon modes preferentially excited nearby QDs, and the radiation of these subpopulations of QDs were subsequently varied through coupling with the nanoprism dipolar resonance at the QDs' emission frequency.[15]

## Conclusions

In conclusion, the NIR QDs/Ag films fabricated by a layer-by-layer approach exhibited significant PL enhancement as compared to Ag-absent QD films. The PL enhancement was dominated by the excitation enhancement when the SPR intensity of the Ag NPs was negligible in the emission wavelength range of QDs. Although both excitation and emission enhancements were expected when the SPR bands were designed to cover both the absorption and emission wavelengths of the QDs, interestingly it was found that the PL enhancement mechanisms and EFs indeed depended on excitation wavelength. No obvious emission enhancement was observed with ~450 nm excitation, while it was clear for 636 nm excitation, as supported by lifetime measurements. It is attributed to the excitation wavelength-dependent coupling efficiency between the related plasmon modes and the QDs. By optimizing the QDs/Ag system, we were able to reach a PL EF as high as 2.8, due to the strong interaction between the QDs and Ag NPs. These QDs/Ag films hold great promise for emerging QD devices for potential applications such as light-emitting diodes and biological sensors.

## Acknowledgements

This work was supported by the funds from the Natural Sciences and Engineering Research Council of Canada and Fonds de la recherche sur la nature et les technologies.

## Notes and references

1 G. Konstantatos, I. Howard, A. Fischer, S. Hoogland, J. Clifford, E. Klem, L. Levina and E.H. Sargent, *Nature,* 2006, **442**, 180.

2 A.L. Rogach, A. Eychmueller, S.G. Hickey and S.V. Kershaw, *Small,* 2007, **3**, 536.

3 E.J.D. Klem, D.D. MacNeil, L. Levina and E.H. Sargent, *Advanced Materials,* 2008, **20**, 3433.

4 V. Giannini, A.I. Fernandez-Dominguez, Y. Sonnefraud, T. Roschuk, R. Fernandez-Garcia and S.A. Maier, *Small,* 2010, **6**, 2498.

5 O. Hess, J.B. Pendry, S.A. Maier, R.F. Oulton, J.M. Hamm and K.L. Tsakmakidis, *Nature Materials,* 2012, **11**, 573.

6 D.R. Jung, J. Kim, S. Nam, C. Nahm, H. Choi, J.I. Kim, J. Lee, C. Kim and B. Park, *Appl. Phys. Lett.,* 2011, **99**, 041906.

7 P.P. Pompa, L. Martiradonna, A. Della Torre, F. Della Sala, L. Manna, M. De Vittorio, F. Calabi, R. Cingolani and R. Rinaldi, *Nat. Nanotechnol.,* 2006, **1**, 126.

8 H. Liang, Z. Li, W. Wang, Y. Wu and H. Xu, *Advanced Materials,* 2009, **21**, 4614.

9 Y. Jiang, H.-Y. Wang, H. Wang, B.-R. Gao, Y.-w. Hao, Y. Jin, Q.-D. Chen and H.-B. Sun, *The Journal of Physical Chemistry C,* 2011, **115**, 12636.

10 T. Ming, H.J. Chen, R.B. Jiang, Q. Li and J.F. Wang, *J. Phys. Chem. Lett.,* 2012, **3**, 191.

11 H. Naiki, S. Masuo, S. Machida and A. Itaya, *The Journal of Physical Chemistry C,* 2011, **115**, 23299.

12 X. Ma, H. Tan, T. Kipp and A. Mews, *Nano Letters,* 2010, **10**, 4166.
13 Y.C. Chen, K. Munechika, I. Jen-La Plante, A.M. Munro, S.E. Skrabalak, Y.N. Xia and D.S. Ginger, *Appl. Phys. Lett.,* 2008, **93**, 053106.
14 K. Munechika, Y. Chen, A.F. Tillack, A.P. Kulkarni, I.J.L. Plante, A.M. Munro and D.S. Ginger, *Nano Letters,* 2010, **10**, 2598.
15 K. Munechika, Y.C. Chen, A.F. Tillack, A.P. Kulkarni, I. Jen-La Plante, A.M. Munro and D.S. Ginger, *Nano Letters,* 2011, **11**, 2725.
16 B.J. Yang, N. Lu, D.P. Qi, R.P. Ma, Q. Wu, J.Y. Hao, X.M. Liu, Y. Mu, V. Reboud, N. Kehagias, C.M.S. Torres, F.Y.C. Boey, X.D. Chen and L.F. Chi, *Small,* 2010, **6**, 1038.
17 K. Tanaka, E. Plum, J.Y. Ou, T. Uchino and N.I. Zheludev, *Physical Review Letters,* 2010, **105**, 227403.
18 H. Zhao, M. Chaker, N. Wu and D. Ma, *Journal of Materials Chemistry,* 2011, **21**, 8898.
19 L. Cademartiri, J. Bertolotti, R. Sapienza, D.S. Wiersma, G. von Freymann and G.A. Ozin, *J. Phys. Chem. B,* 2006, **110**, 671.
20 H. Zhao, M. Chaker and D. Ma, *Journal of Physical Chemistry C,* 2009, **113**, 6497.
21 Q.A. Zhang, W.Y. Li, L.P. Wen, J.Y. Chen and Y.N. Xia, *Chemistry-a European Journal,* 2010, **16**, 10234.
22 H.L. Liang, W.Z. Wang, Y.Z. Huang, S.P. Zhang, H. Wei and H.X. Xu, *The Journal of Physical Chemistry C,* 2010, **114**, 7427.
23 H. Liang, H. Yang, W. Wang, J. Li, H. Xu, *Journal of the American Chemical Society,* 2009, **131**, 6068.
24 H.Y. Liang, H.G. Zhao, D. Rossouw, W.Z. Wang, H.X. Xu, G.A. Botton and D.L. Ma, *Chemistry of Materials,* 2012, **24**, 2339.
25 T.R. Dhakal, S.R. Mishra, Z. Glenn and B.K. Rai, *J. Nanosci. Nanotechnol.,* 2012, **12**, 6389.
26 Z. Liu, H. Zhou, Y.S. Lim, J.H. Song, L. Piao and S.H. Kim, *Langmuir,* 2012, **28**, 9244.
27 A.Q. Chen, A.E. DePrince, A. Demortiere, A. Joshi-Imre, E.V. Shevchenko, S.K. Gray, U. Welp and V.K. Vlasko-Vlasov, *Small,* 2011, **7**, 2365.
28 S.J. Barrow, A.M. Funston, D.E. Gomez, T.J. Davis, P. Mulvaney, *Nano Letters,* 2011, **11**, 4180.
29 H.X. Xu, E.J. Bjerneld, M. Kall and L. Borjesson, *Physical Review Letters,* 1999, **83**, 4357.
30 Y. Yang, J. Shi, T. Tanaka and M. Nogami, *Langmuir,* 2007, **23**, 12042.
31 F.P.G. de Arquer, F.J. Beck, M. Bernechea and G. Konstantatos, *Appl. Phys. Lett.,* 2012, **100**, 043101.